Triton
Tank Test Report

DE-FOA-0001310: Next Generation Marine Energy Systems - Durability & Survivability
Award Number: DE-EE0007346
Principle Investigator: Tim Mundon. Ph.D.
Submission Date: September 28, 2018

Document contributes towards M6, D9

Following drawings provided:
<D6_Tank_Test_Plan_Drawings.pdf>

1. Table of Contents:

2. Summary / Scope

This report summarizes results from physical model testing of the Triton WEC. Tank tests were performed at 1:30 scale in the large wave flume at the OSU Hinsdale Laboratory.

References

D6_Tank_Test_Plan.docx
D6_Tank_Test_Plan_Waves.xlsx
D6_Tank_Test_Plan_Instrumentation_List.xlsx
D6_Tank_Test_Plan_Drawings.pdf

3. Summary

OPI successfully completed all planned tests detailed in the Tank Test Plan Report. There were no serious issues during the testing, only a few temporary instrumentation failures that were corrected and the failed test repeated. A chronological list of tests and a Quality Control log are presented in "D6_Tank_Test_Plan_Waves.xlsx".

The model Triton was tested over a range of realistic irregular seas, in both the floating (operational) configuration and the submerged (survival) configuration. The largest wave conditions tested were representative of the 1:50 year design envelope at the hypothetical deployment location selected for this project, Humboldt Bay CA. In addition to the extreme conditions, specific focus was placed on the Triton performance in large operational waves, near the threshold at which the system can survive in the floating (operational) configuration. Further, a set of monochromatic and focused waves were tested to validate both system hydrodynamics and the CFD simulations performed as part of this project. These results are presented in the Numerical Survivability Report.

A summary of the key findings from the physical model testing:

- The mid-fidelity OrcaFlex model provided good predictions of maximum loads. Peak tendon tension loads were accurate to within 3%. Peak mooring loads were accurate to within 27%[1].
- In the same sea state, submerging the system under the surface reduces the peak tendon tension fluctuations by 50% and the peak PTO displacement fluctuations by 70%.
- The submerged strategy saw no end-stop events or slack events in any conditions along the 1:50 year contour.
- In large survival seas, the system experiences wave driven second order drift loads that provide a net upward drift force. This is an effect not observed in previous numerical work and needs further investigation to understand and quantify. In smaller survival seas, this effect is minimal and results remain consistent with earlier numerical simulations.
- The maximum submergence depth observed in the physical model tests (approximately 25m) is slightly lower than, although in line with, prior numerical predictions. However it should be noted that achieving the exact negative buoyancy was challenging, and may have contributed to any mismatch in submergence depth.

[1] A significant portion of this discrepancy may be attributed to the challenge and inability to perfectly represent the mooring arrangement in the tank tests, described further in Section 5.

4. Physical model

A description of the 1:30 physical model designed, constructed and tested for this project is presented in this section.

Figure 1. *1:30 model Triton at OSU*

Model construction

The surface float is 3D printed as a hollow shell and reinforced with an outer layer of fiberglass and epoxy. High density inserts are incorporated to serve as interfaces for mounting the PTO and mooring lines. The float is fitted with lifting eyes for installing the device as well a sealed top hatch to eliminate water ingress during testing and to allow the PTO to be accessed and modified between tests. The reaction ring is 3D printed from 12 ABS plastic sections that are bolted together and lead ballasted.

The tendons that connect the surface float and reaction ring are 2 mm UHMWPE line. Three bellmouth fairleads, 3D printed from a self-lubricating material, are incorporated into to the surface float to align each tendon with the PTO.

Representative PTO

The 1:30 Triton model contains three representative power take-offs (PTOs), housed inside the surface float, one for each of the three tendons (Figure 2). Each drivetrain comprises a spring-damper element consisting of an extension spring, to support the weight of the reaction ring, and a rotary oil dashpot, to represent the power absorption (generator).

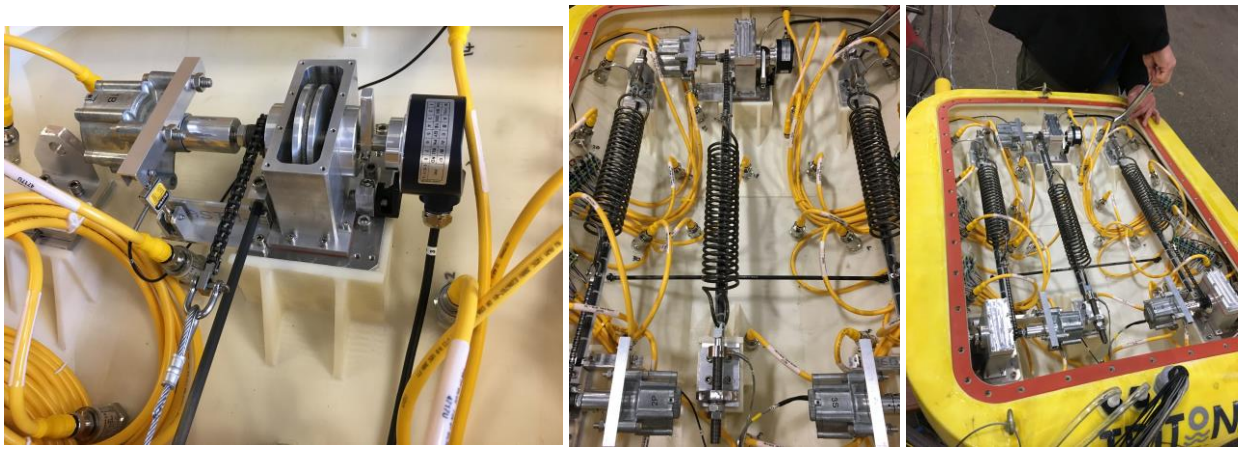

Figure 2. *Model drivetrain and instrumentation. Bow PTO with encoder and damper shown on top with other images showing layout of return springs and pressure transducers, bottom.*

The linear displacement and force exerted by the relative motion of the reaction ring and surface float is translated to rotary motion by the tendon wrapping once around a sheave (D = 60 mm). A rotary damper, produced by Kinetrol (S-CRD, 100000 cSt) is directly attached to the sheave's axle. This unit dissipates energy by shearing viscous fluid (silicone oil) between rotor and stator discs. A chain/sprocket assembly is used to convert the sheave rotary motion back into linear motion for the extension spring. The gear ratio between the sheave and sprocket is 2.45.

The full-scale Triton WEC has mechanical end-stops that limit the tendon's linear travel to 3m (peak to peak). Representative hard end-stops in the 1:30 model are provided by a cam mechanism attached to the sheave axle. After the sheave revolves ± 95 degrees, the cam hits a rubber pad, causing the PTO motion to be restrained.

The oil dashpot was selected such that it produces similar damping characteristics as the full-scale Triton generator. Additionally, the damper is adjustable so that its damping can be tuned to the optimal value for each wave condition, as would be done in practice. The three dampers were thoroughly tested in the OPI laboratory to confirm that they provide suitably linear force-velocity characteristics, as shown in Figure 3. Additionally, the mechanical extension springs were calibrated to ensure that their spring rate was known accurately.

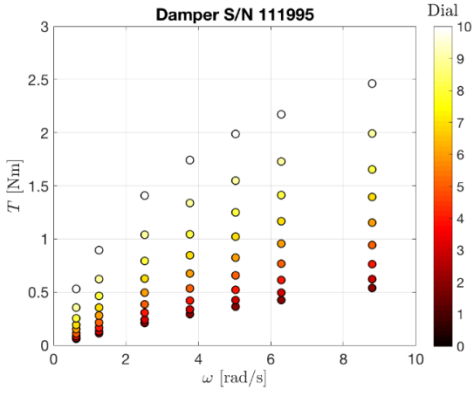

Dial	Model-scale (rotary) damping [Nm/rad/s]
2	0.067
3	0.078
4	0.096
5	0.120
6	0.149
7	0.182
8	0.221
9	0.272
10	0.345

Figure 3. *(Left) Kinetrol S-CRD rotary damper. (Center-Right) Adjustable model damper characteristics*

Experiments performed in large operational and extreme waves were conducted using "stiff" spring-damper settings that closely match the limits of the realistic Triton PTO. Experiments in smaller operational waves were performed using softer spring and damper settings that are also representative of a typical operating point for the Triton PTO.

Instrumentation

A detailed channel list is provided in "D6_Tank_Test_Instrumentation_List.xlsx". Drawings of the instrument locations are provided in "D6_Tank_Test_Plan_Drawings.pdf".

The physical model contains 48 analog sensors

- 31 differential pressure transducers for measuring the surface float pressure distribution and green water loads
- 14 load cells
    - *Tendon force* (for each of the 3 tendons): A submersible load cell is attached between each tendon and the reaction ring using shackles
    - *Spring force* (for each of the 3 drivetrains): A load cell is placed in line with each of the extension springs
    - *Damping force* (for each of the 3 drivetrains): The body of each rotary damper is restrained from moving at a single point by a torque arm. This point had a tension and compression load cell installed. The length of the torque arm is 55 mm.
    - *End-stop force* (for each of the 3 drivetrains): A load cell placed under the rubber end-stop is used to measure the end-stop force for each PTO
    - *Mooring force* (for each of the 2 mooring legs): Submersible load cells are attached between the surface float and the upper bow and stern mooring lines.
- The model contains 3 optical rotary encoders to measure the displacement of each of the drivetrain sheaves. OPI used a quadrature to analogue converter to convert the digital signals to -5 V to 5 V.

The instrumentation cable bundle is passed out the rear of the hull through a sealed gland.

Motion capture (XYZRPY) of the surface float is performed using the OSU PhaseSpace system. An IMU is installed on the reaction structure to measure its motion. All motion, instrumentation, and wave data are sampled on a concurrent time basis.

Hull pressurization system

Due to the numerous hull penetrations, namely the access hatch and the pressure transducers, a positive pressure system was incorporated in the surface float to prevent water ingress. A manual pressure regulator (connected to a large air reservoir) was used to pressurize the surface float and maintain an internal pressure of approximately 0.5 psig for operational (floating) tests and approximately 1.5 psig for survival (submerged) tests. The regulator was located outside of the flume and was connected to the surface float with a small flexible pressure tube. This tube was incorporated into the instrumentation bundle to minimize impact on device motions.

Since the pressure transducers are differential, the vents from all 31 transducers were connected to a manifold and vented out of the surface float through a second flexible tube exposed to atmospheric pressure.

The hull pressurization worked successfully and there was no observation of water entry during the test campaign.

Ballasting for survival configuration

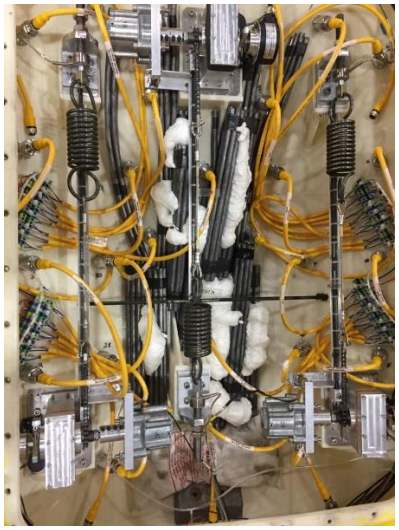

Figure 4. *Lead ballast used to submerge the system.*

To replicate the submerged survival mode, the model surface float was manually ballasted with lead until the system submerged below the surface and was supported by the mooring floats. Achieving the required submergence depth was difficult as this was found to be very sensitive. Only an approximate match to the required depth was possible, however this is not expected to have influenced the results significantly. A total of 60.5 kg of lead was used, which corresponds to ~1600 tonnes at full scale. This is in line with estimates for the amount of water required to perform the ballasting operation for a full-scale Triton (~1500 tonnes).

Representative mooring

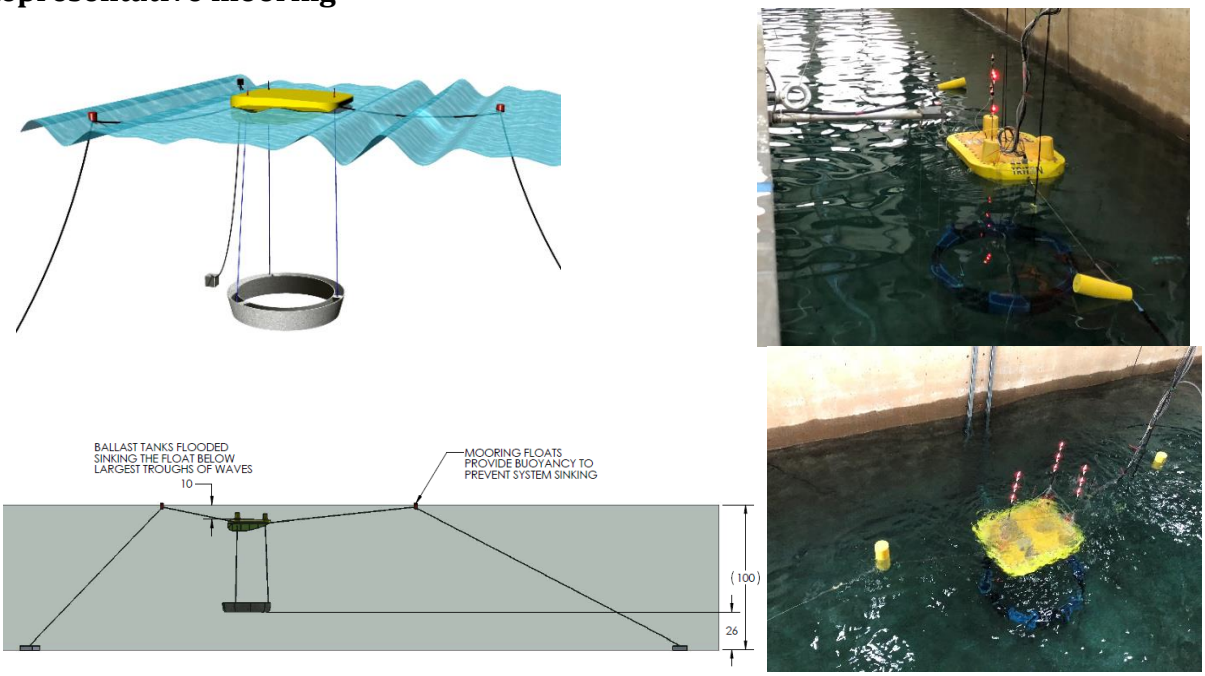

Figure 5. *Floating and submerged mooring configurations. A realistic 3-point mooring is shown on the left, and the laboratory mooring configuration is shown on the right.*

The constraints of completing these tests in a flume (which was required due to availability and wave height demands) presented some challenges to perfectly replicating the Triton mooring system. Due to the width of the OSU flume, the mooring was modified from a three-point configuration (Figure 5) to a two-point (bow and stern) configuration. An additional, minor, contributing factor to the laboratory mooring design was that the OSU flume was representative of an 80m depth (flume depth = 2.7m), while the numerical simulations in this project were performed at a 120m depth.

Therefore, careful attention was given to ensure that the laboratory two-point mooring provided the same effective stiffness as the realistic three-point arrangement. OrcaFlex was used to validate the laboratory mooring arrangement and to determine appropriate line elasticities that would give the correct mooring force-displacement profile. Appropriate mechanical springs were then selected and introduced in the upper and lower lines for the 1:30 model tests. Due to the reduction to two mooring legs, separate mooring arrangements were needed for the operational and survival configurations, summarized in Table 1.

Table 1. *Mooring properties used in the tank tests*

	Operational (Floating)	Survival (Submerged)
Upper Line Total Length	1.67 m	1.67 m
Upper Line Material	Spectra + Steel Spring (k=1.1 lb/in)	Spectra
Lower Line Total Length	8.21 m	8.8 m
Lower Line Material	Spectra + Rubber Spring (k = 0.2 lb/in)	Spectra + Steel Spring (k = 1.1 lb/in)
Anchor Diameter	20 m	20 m
Mooring float buoyancy	0.0015 m^3	0.0015 m^3

Figure **6** shows the effective horizontal mooring stiffness (in operational mode) and the effective vertical mooring stiffness (in submerged mode) achieved in OrcaFlex for the realistic and laboratory arrangements, demonstrating good agreement.

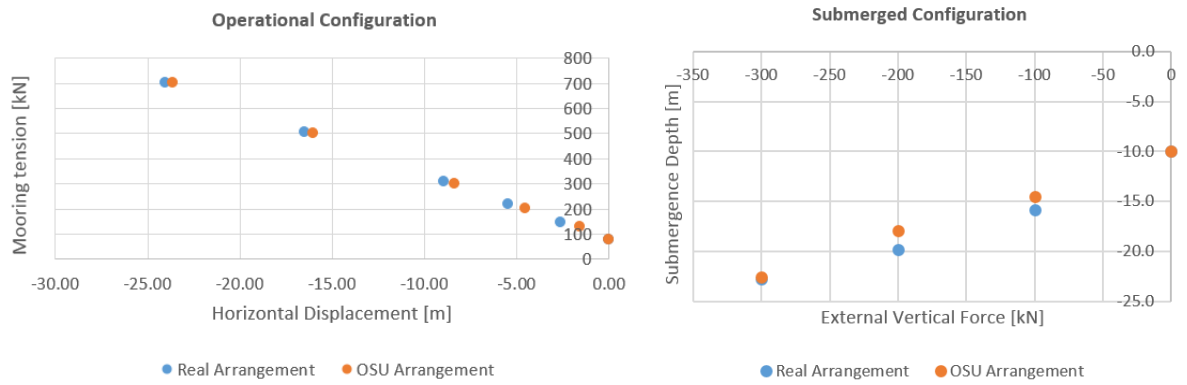

Figure 6. *Effective stiffness (at full-scale) for realistic and laboratory mooring configurations.*

Test facility and model installation

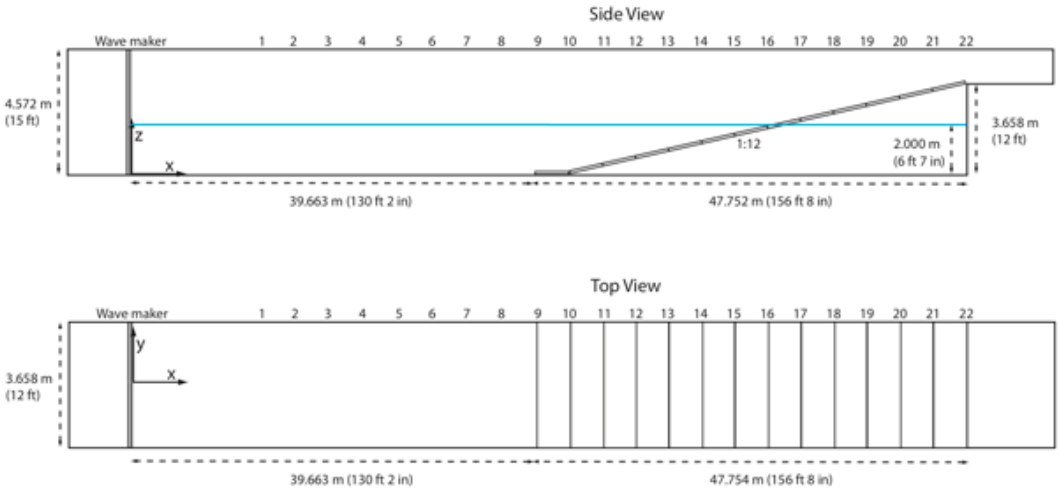

Figure 7*. OSU Large Wave Flume [courtesy of OSU]*

Tests were conducted at the Oregon State University Large Wave Flume. The flume width is 3.7m and the (still) water depth is 2.7m.

Four measurements of wave elevation were made using resistive wave gauges: 2 upwave of the device, 1 at the device location, and 1 downwave of the device. Wave probes were 35 cm away from the basin sidewalls (the lateral uniformity of the waves is acceptable and therefore the probes do not need to be centered in the flume). These wave probes were in place during device testing and calibration (no device in flume). Wave

calibrations were performed prior to model testing to ensure accuracy of T_p and H_s to within 5%. All waves were tested at 0° incidence to the physical model. The locations of the wave gauges and the Triton model are summarized in Table 2.

Table 2. *Model and wave gauge positions*

	Downwave (x) distance from wave paddle [m]
1:30 Triton Model	25.1
Wave Gauge 1	17.8
Wave Gauge 2	21.5
Wave Gauge 3	25.1
Wave Gauge 4	28.8

5. System design loads

Maximum operational contour

The results from the mid-fidelity modeling work, which are summarized in the Numerical Survivability Report, report that the maximum mooring and tendon (and hence drivetrain) loads occur when the WEC is on the surface. This modeling work also reports that there is wave height threshold at which the system can safely remain on the surface, without experiencing potentially harmful slack events and end-stop events. Beyond this threshold, the system must be submerged in order to avoid these events.

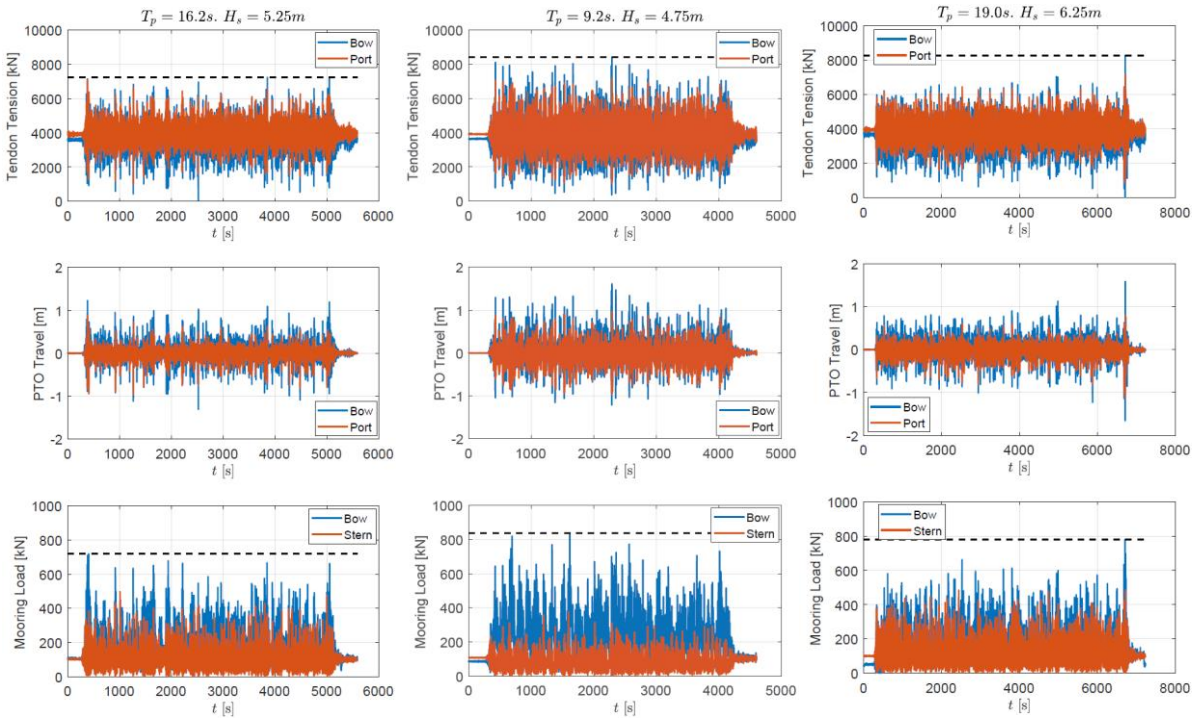

Figure 8. *System loads on maximum operational wave contour.*

Figure 8 shows system performance for three wave condtions along this maximum operational contour. It can be seen that the PTO travel is kept to within the 3m limitation, thus avoiding end-stops, and that the tendons remain in tension. There is one slack/snap event that occurs during the longest period operational wave condition (T_p=19.0s, H_s=6.25m), which can likely be mitigated by slightly lowering the threshold condition for entry to the survival configuration in longer wave periods (<16s).

Comparison to numerical model

Table 3 and Table 4 demonstrate that the maximum tendon tensions and mooring tensions measured in the physical model agree well with the OrcaFlex results. The maximum tendon tensions can be seen to agree particularly well, to within 2.5%.

Table 3. *Tendon loads on maximum operational wave contour. Physical model results versus OrcaFlex simulation results. *Slack/snap event was removed.*

T_p [s]	H_s [m]	Test #	Maximum Tendon Tension [kN]		% Difference
			1:30 Experiments	OrcaFlex Simulation	
9.2	4.75	WT16	8400	8530	1.6%
16.2	5.25	WT17	7220	7040	-2.5%
19.0	6.25	WT18	7030*	7000	-0.4%

Table 4. *Mooring loads on maximum operational wave contour. Physical model results versus OrcaFlex simulation results.*

T_p [s]	H_s [m]	Test #	Maximum Mooring Tension [kN]		% Difference
			1:30 Experiments	OrcaFlex Simulation	
9.2	4.75	WT16	840	950	13%
16.2	5.25	WT17	720	900	25%
19.0	6.25	WT18	780	990	27%

With any scaled physical model, it is challenging to perfectly replicate every parameter and moorings can be particularly sensitive. Some differences between the full-scale prototype (OrcaFlex) and the physical model are noted below:

- In this model, to approximately achieve the correct elasticity for the lower mooring line segment, a soft rubber cord was used. While metal mechanical springs are typically more ideal in this application due to their more linear characteristics, the rubber cord was the only practical option. Unfortunately, it was slightly stiffer at low displacement and slightly softer at large displacements, which may help explain why the experiments yielded slightly lower mooring tension maxima.

- In the physical model tests, the upper mooring line segments had to be shortened by approximately 10% to achieve the correct mooring pretension. This required adjustment was possibly due to the tolerances on the achieved anchor locations.
- In addition to these differences in the mooring properties, there are some second-order physical parameters that are not known a priori and must be approximated in the OrcaFlex model. These include, for example, line damping (especially important as we used rubber springs) and the hydrodynamic drag of the floats and lines.

Given these considerations, the agreement in the maximum mooring tensions, within 27%, is fairly reasonable.

6. Submerged survival strategy

Demonstration of load reduction

For two of the same three wave conditions, Figure 10 compares the performance when the system is floating versus submerged. It is clear that sinking the system below the surface significantly detunes the system, resulting in lower tendon tensions and drivetrain travel. As summarized in Table 5, on average, the maximum tendon tension fluctuation reduced by 50% and the maximum PTO travel reduced by 70%.

Figure 9. *Model in the operational configuration (left) and submerged (right)*

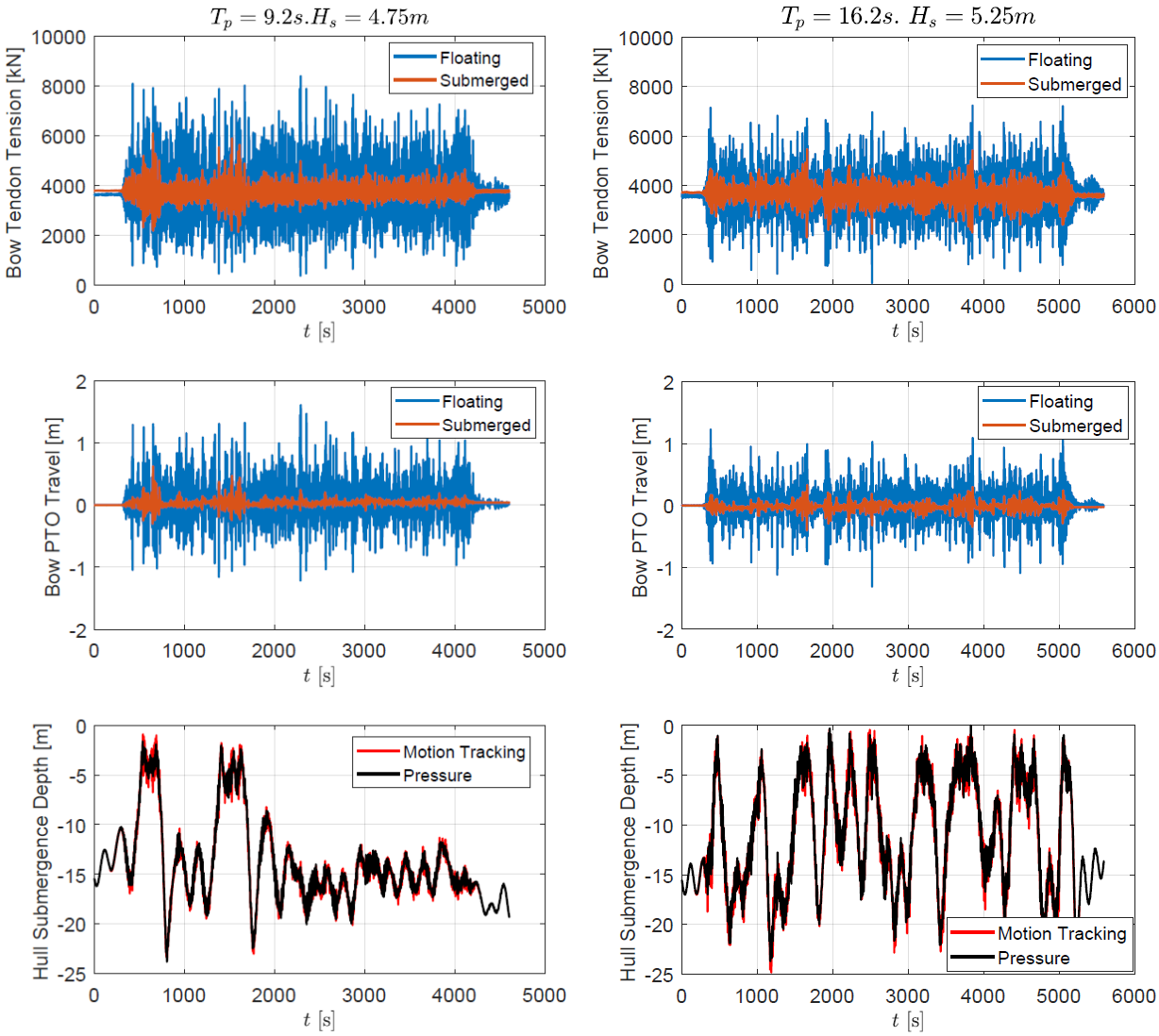

Figure 10. *System dynamics in floating and submerged for the same wave condition.*

Also shown are time traces of the hull depth when in submerged survival mode. The hull depth was measured using two different methods. The first method is an optical measurement using the PhaseSpace motion capture system. The second method relies on inferring the hull depth from the hydrostatic pressure measured by one of the pressure transducers. The two methods are compared and demonstrate excellent agreement.

When the system is submerged, there is a clear correlation between the level of system loading and submergence depth. This is particularly clear for T_p = 9.2s, H_s= 4.75m at t = 500-600s and at t=1500-1700s as shown in Figure 10. During both of these periods, the tension and displacement fluctuations are clearly higher when the hull is closer to (or at) the surface. While it can be seen that there is significant attenuation of system response at >5m submergence depths, the system response at 0m is still substantially reduced from the operational configuration.

Another observation is that the submerged system vertically oscillates with a very slow period, on the order of 200s, consistent with observations from OrcaFlex. This is due to the large system inertia coupled with the soft vertical restoring spring provided by the mooring. The maximum submergence depth, on the order of 20-25m, is in line with predictions provided by OrcaFlex.

Table 5. *Physical model results for floating (operational) model versus submerged (survival) mode.*

T_p = 9.2s, H_s = 4.75m				
Quantity	**Configuration**	**Test #**	**Value (pk-pk)**	**% Reduction**
Bow Tendon Tension Fluctuation, peak-to-peak [kN]	Floating	WT16	8030	
	Submerged	WT23	3960	51%
Bow PTO Displacement Fluctuation, peak-to-peak [m]	Floating	WT16	2.82	
	Submerged	WT23	0.92	67%
T_p = 16.2s, H_s = 5.25m				
Quantity	**Configuration**	**Test #**	**Value (pk-pk)**	**% Reduction**
Bow Tendon Tension Fluctuation, peak-to-peak [kN]	Floating	WT17	7160	
	Submerged	WT24	3560	50%
Bow PTO Displacement Fluctuation, peak-to-peak [m]	Floating	WT17	2.54	
	Submerged	WT24	0.73	71%

Performance in 1:50 year waves

Figure 11 shows Triton performance in survival mode in 1:50 year waves. It can be seen that the system is able to survive these waves with no end-stop events (i.e. the PTO travel is within 3m) and minimal slack events.

Interestingly, in these larger waves, the system appears to migrate towards the surface and tends to stay there, with the deck slightly submerged and the drivetrain housings above the water line. This effect is likely due to second order mean drift loads, which were not previously accounted for and will need to be investigated further in order to improve the fidelity of the numerical model. It is likely that this effect is also a contributing factor in the discrepancy in mooring loads (compared to the numerical model) in the 1:50 year waves.

This behavior is in contrast to the smaller waves where the system experiences dramatic variations in submergence depth. This is presumably because the second order mean drift forces only become dominant compared to the buoyancy forces in the larger waves.

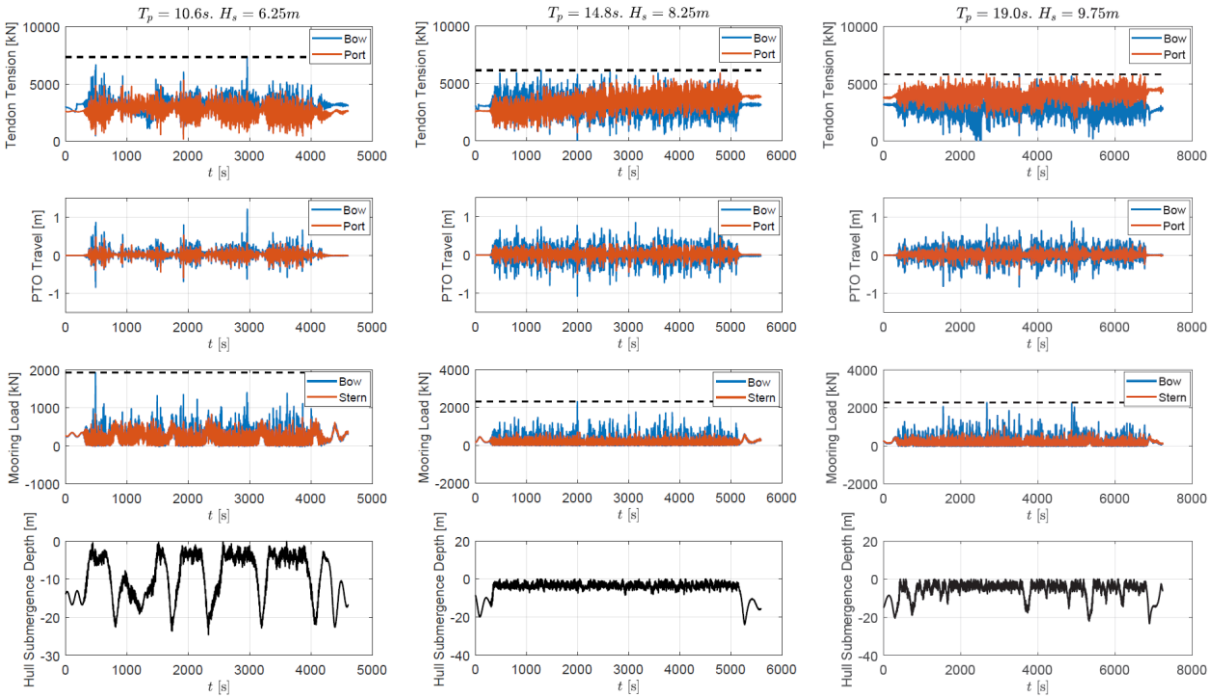

Figure 11. *System loads in submerged mode in 1:50 year waves.*

7. Conclusions

Maximum submergence depth

The structural loads on the hull are dominated by the hydrostatic loads in the submerged survival configuration. Figure 12 indicates how the submergence depth impacts the cost.

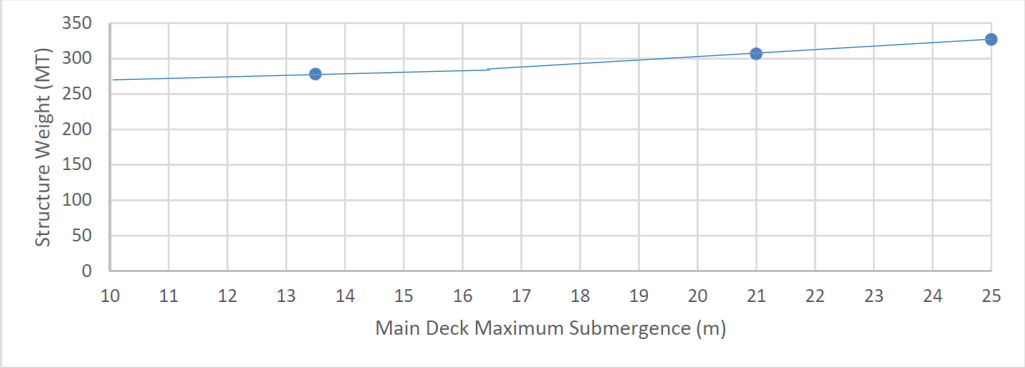

Submergence Depth	Structure Weight MT	Structure Cost -	Difference in Cost
Deep	326.81	$937,000	-
Medium	306.55	$879,000	-6%
Shallow	278.05	$797,000	-15%

Figure 12. *Steel structural cost vs maximum submergence depth.*

The physical model tests indicate that the maximum submergence of the hull will be 22m indicating an approximate structure mass of 310MT. However, the results also indicate that we may be able to improve the strategy in order to reduce the maximum submergence depth.

Further design improvements

Figure 11 shows that even when the system is close to the surface, such that the upper extremities of the hull are just above the waterline, the loads are still mitigated significantly compared to the maximum operational conditions. This is likely due to the fact that the ballasted mass of the float substantially reduces the response of the system compared to the operational configuration. Accordingly, we may conclude that a full submergence may not be required, and a potential strategy is to retain some minimal reserve buoyancy (1-2%) within the float. This would mitigate the long period vertical oscillation that was observed and allow the structural cost of the hull to be reduced. However, in this case, as indicated by the physical model, the mooring loads would be increased and the impact of this on the design would need to be assessed.